

Chromium wheels *quasi-hexagonal* 2D assembling by direct UHV sublimation.

Marzio Rancan,* Francesco Sedona, Marco Di Marino, Lidia Armelao and Mauro Sambi

Electronic Supplementary Information

1. Synthesis

Reagents were purchased from Aldrich and used as received unless otherwise stated. The starting material $\{[\text{Cr}_6\text{F}_7(\text{O}_2\text{CCMe}_3)_{10}][\text{NH}_2\text{Et}_3]_3\}_2$ has been prepared as reported in literature.¹ Fe(III) wheels $\{\text{Fe}_{10}(\text{OMe})_{20}(\text{O}_2\text{CR})_{10}\}$ ($\text{R} = \text{CMe}_3, \text{Ph}$) have been synthesised by methanolysis of the parent iron (III) basic carboxylate in presence of NEt_3 as reported by Christou *et. al.*² working in a glove box atmosphere. The nature of starting materials and iron wheels has been confirmed by elemental analysis.

1.1 $\{\text{Cr}_{10}(\text{OMe})_{20}(\text{O}_2\text{CCMe}_3)_{10}\}$ has been synthesized by a solvothermal reaction similar to that reported by McInnes *et. al.*³ using $\{[\text{Cr}_6\text{F}_7(\text{O}_2\text{CCMe}_3)_{10}][\text{NH}_2\text{Et}_3]_3\}_2$ as starting material. 300 mg of the parent compound dissolved in 10 of MeOH was placed in a Teflon-lined vessel and heated under autogenous pressure to 150°C for 24 h and cooled to room temperature over a period of 16 h. Dark-green crystals of the compound deposited during the cooling (yield 60 %). Crystals have been collected and recrystallized from toluene and characterized by X-ray single crystal. Elemental analysis: calc (%): C 38.9, H 6.9; exp (%): C 39.2, H 7.1.

2. Bulk $\{\text{Cr}_{10}\}$ characterization

2.1 Structural characterization

The $\{\text{Cr}_{10}\}$ structure has already been reported,³ crystallization from toluene leads to a different unit cell parameters due to the presence of solvent molecules. $\{\text{Cr}_{10}\} \cdot 2(\text{C}_7\text{H}_8)_2$ X-ray quality single crystals were grown over one week from a 10^{-4} mol/L toluene solution. The selected crystal ($0.4 \times 0.2 \times 0.1$ mm) was mounted on the top of a Lindemann glass capillary using Paratone-N oil and centred on the four-circle kappa goniometer head of an Oxford Diffraction Gemini E diffractometer, equipped with a $2\text{K} \times 2\text{K}$ EOS CCD area detector and sealed-tube Enhance (Mo) and (Cu) X-ray sources, under a cold nitrogen stream provided by an Oxford Instruments CryojetXL sample chiller. Data were collected by means of the ω - scans technique ($3.04^\circ < \theta < 26.53^\circ$) at $T = 150.0(1)$ K and using graphite-monochromated Mo K_α radiation ($\lambda = 0.71073$ Å), in a 1024×1024 pixel mode, using 2×2 pixel binning. The diffraction intensities were corrected for Lorentz and polarization effects and were also optimized with respect to absorption. Empirical multi-scan absorption corrections using equivalent reflections were performed with the scaling algorithm *SCALE3 ABSPACK*. Data collection, data reduction and finalization were carried out through the

CrysAlisPro software.⁴ Accurate unit cell parameters were determined during the whole data collection by least-squares refinement of all reflection positions. Crystal stability was checked by measuring in both cases two reference frames after every 50 frames; no sign of systematic changes was noticed neither in peak positions nor in intensities.

The structure was solved by means of the direct methods using SHELXS⁵ and refined by full-matrix least-squares methods based on F_o^2 with SHELXL-97⁵ in the framework of OLEX2⁶ software. {Cr₁₀} crystallized with two toluene molecules; the asymmetric unit contains half the wheel and one solvent molecule, with the other half and the other toluene molecule related by a symmetry element. The methyl groups C(1), C(2), C(3), C(34) and C(35) were disordered over two sites, the occupancies of which were constrained to sum to 1.0. The thermal motion of the C1s, C6s and C7s in the solvent molecule were high and attempts were made to split these atoms into two disordered components, but no acceptable models could be obtained. Therefore, they were not split in the final refinement. With the exception of disordered atoms, all non-H atoms were refined anisotropically in the last cycles of refinement. H atoms were included in calculated positions in the final model, with the exception of the disordered C(34) and C(34A) atoms. Crystal data and structure refinement are displayed in Table S1, CCDC 811743.

Table S1

Empirical formula	C ₈₄ H ₁₆₀ Cr ₁₀ O ₄₀
Formula weight	2336.15
Temperature / K	150(1)
Crystal system	triclinic
Space group	P-1
a/Å, b/Å, c/Å	9.914(5), 17.909(5), 18.644(5)
α / °, β / °, γ / °	117.67(1), 102.63(1), 94.05(1)
Volume/Å ³	2804(2)
Z	1
ρ _{calc} /mg mm ⁻³	1.380
μ/mm ⁻¹	1.005
F(000)	1224
Crystal size/mm ³	0.4 × 0.2 × 0.1
θ range for data collection	3.04 to 25.55°
Index ranges	-12 ≤ h ≤ 11, -21 ≤ k ≤ 22, -23 ≤ l ≤ 23
Reflections collected	31323
Independent reflections	9873[R _{int} = 0.0455]
Data/restraints/parameters	9873/607/629
Goodness-of-fit on F ²	1.050
Final R indexes [I>2σ (I)]	R ₁ = 0.0465, wR ₂ = 0.1280
Final R indexes [all data]	R ₁ = 0.0703, wR ₂ = 0.1479
Largest diff. peak/hole/e Å ⁻³	1.067/-0.637

Table S1. Crystal data and structure refinement for $\{\text{Cr}_{10}\} \cdot 2(\text{C}_7\text{H}_8)_2$.

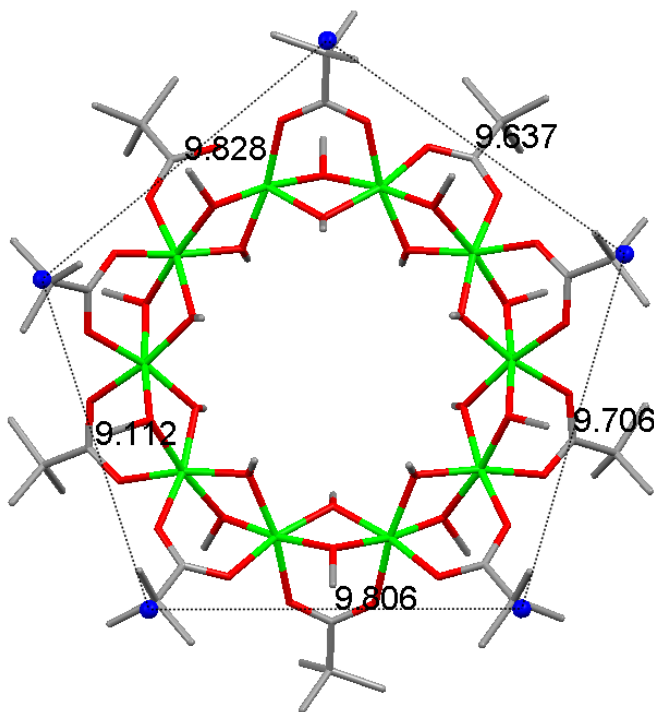


Fig. S1. $\{\text{Cr}_{10}\}$ capped-sticks structure. Blue spheres: “ $\text{C}(\text{CH}_3)_3$ ” centroids. Black dashed-lines: distances (\AA) among centroids. Atoms colour code: Cr green, O red, C grey.

Distances among the tert-butyl groups have been determined calculating each “ $\text{C}(\text{CH}_3)_3$ ” centroid (blue spheres, Fig. S1) with Mercury 2.3 software. Distances are displayed in Fig. S1: the mean value is 9.6 \AA .

2.2 X-Ray Photoelectron Spectroscopy of bulk $\{\text{Cr}_{10}\}$

XPS spectra were recorded on a Perkin–Elmer Φ 5600ci spectrometer using a non-monochromatized (15 kV, 300 W) Al K α radiation (1486.6 eV). The sample analysis area was 2 mm in diameter, and the working pressure was lower than 10^{-9} mbar. The spectrometer was calibrated assuming the binding energy (BE) of the Au4f $_{7/2}$ line at 83.9 eV with respect to Fermi level. The standard deviation for the BEs was ± 0.15 eV. Bulk crystalline $\{\text{Cr}_{10}\}$ was mounted on a steel sample holder and introduced directly into the XPS analytical chamber by a fast entry lock system. Survey scan (Fig. S2) has been run in the 0–1250 eV range to identify the chemical species present in the sample. Detailed scans were recorded for the C1s, O1s and Cr2p photo-peaks (Fig. S3). For bulk $\{\text{Cr}_{10}\}$, BE shifts due to charging effects were corrected assigning the adventitious C1s line at BE of 285.0 eV.⁸ The analysis involved Shirley-type background

subtraction and, whenever necessary, spectral deconvolution, which was carried with XPSPEAK 4.1 program. C1s signal can be properly deconvoluted into three spectral components: the dominant, lower energy component (C_I) ascribed to aliphatic carbon in the tert-butyl groups and to the adventitious carbon,⁹ component C_{II} associated to oxygen-bound carbon of methoxy groups (OC^*H_3)⁹ and component C_{III} assigned to the electron-depleted carbon of carboxylate groups (C^*OO).⁹ The atomic composition of the sample was calculated by peak integration, using sensitivity factors provided by the spectrometer manufacturer (Φ V5.4A software) and taking into account the geometric configuration of the apparatus. The experimental uncertainty on the reported atomic composition values does not exceed $\pm 5\%$. The results of the analysis are gathered in Tables S2-S4. The atomic ratio O/Cr and C_{II}/C_{III} are in very good agreement with the nominal values for $\{Cr_{10}\}$.

Table S2

Bulk $\{Cr_{10}\}$	BE (eV)	FWHM (eV)	% at.
$Cr3p_{3/2}$	577.6	3.4	19 %
O1s	532.2	2.8	81 %
C1s	285.4	2.8	†

† not considered since affected by adventitious carbon

Table S2. XPS data recorded on bulk $\{Cr_{10}\}$.

Table S3

C1s Bulk $\{Cr_{10}\}$	BE (eV)	FWHM (eV)	% at.
C_I	285.0	2.4	†
C_{II}	286.1	2.4	68
C_{III}	288.6	2.8	32

† not considered since affected by adventitious carbon

Table S3. Deconvolution of C1s XPS peak recorded on bulk $\{Cr_{10}\}$.

Table S4

Atomic ratio	Nominal [§]	Bulk $\{Cr_{10}\}$
O/Cr	4	4.2
C_{II}/C_{III}	2	2.1

[§] $\{Cr_{10}[OC_{II}H_3]_{20}[O_2C_{III}C_I(C_IH_3)_3]_{10}\}$

Table S4. Atomic ratio from XPS recorded on bulk {Cr₁₀}.

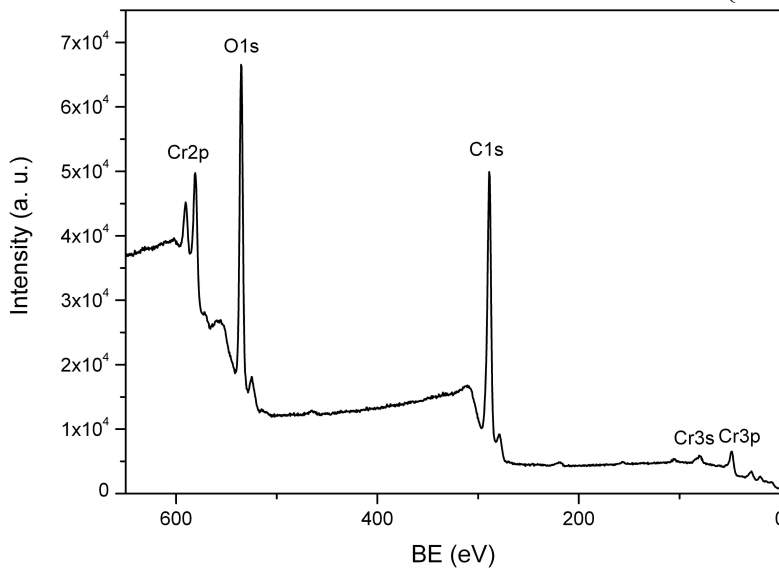


Fig. S2. XPS survey of bulk {Cr₁₀} in the 0-650 eV region.

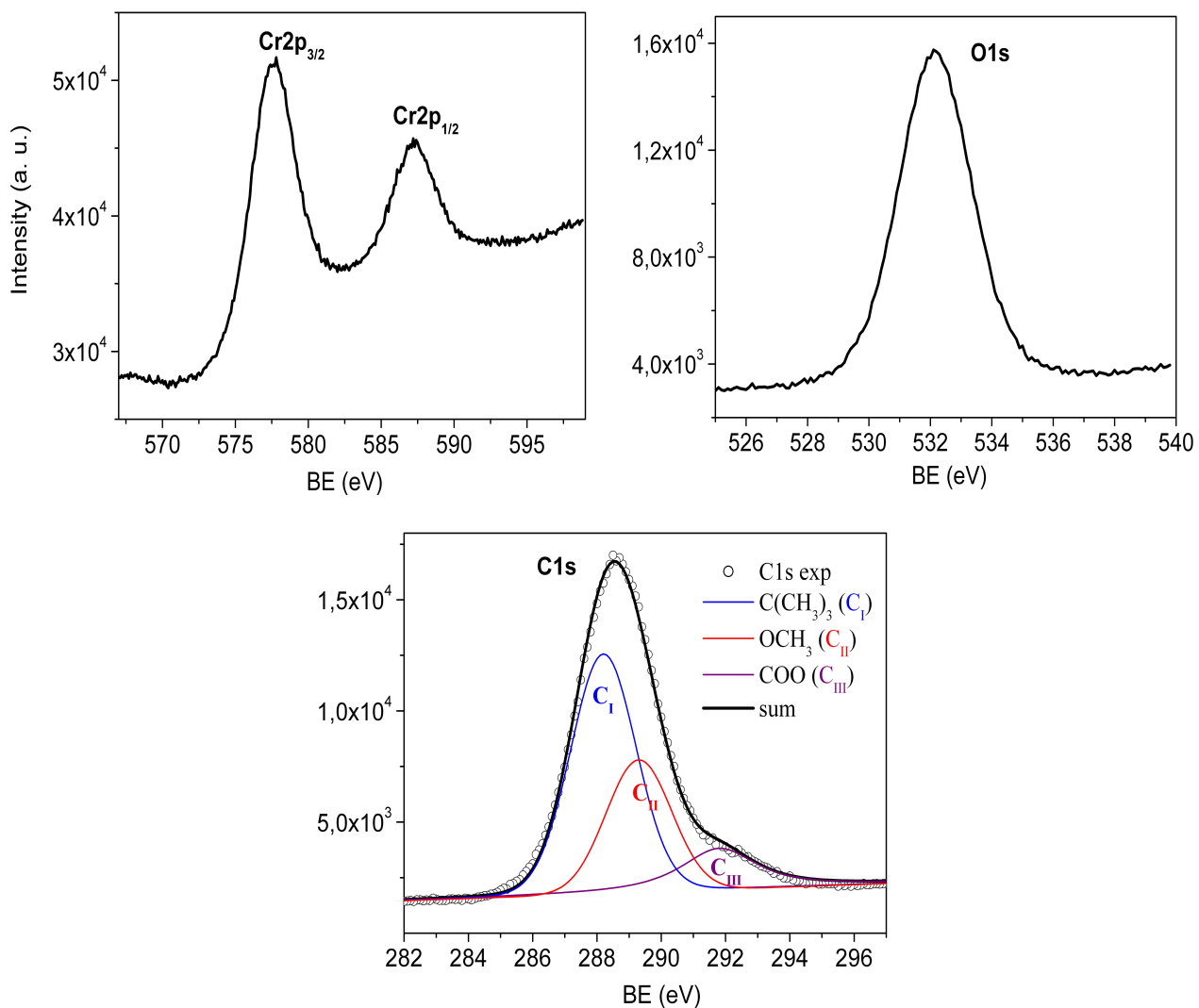


Fig. S3. XPS Cr_{2p}, O_{1s}, C_{1s} regions of bulk {Cr₁₀} and best fit profiles for C_{1s}.

3. TGA analysis

Thermal analyses were performed using a SDT 2960 apparatus from TA Instruments. The weight of the used samples was in the range 8-12 mg. Data were recorded under N₂ flow, with a heating rate of 10 °C/min. Isothermal TGA studies were carried out at ambient pressure and at temperature lower than 350 °C to ensure a higher compound stability.

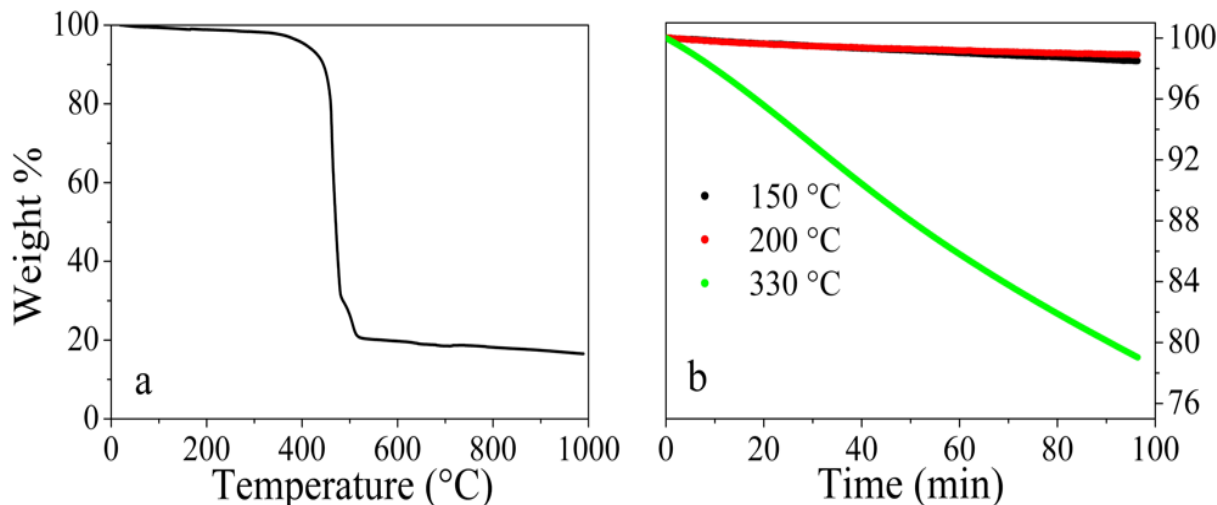


Fig. S4 {Cr₁₀} TGA (a) and isothermal behaviour (b) under N₂ flow.

Centered at 450 °C there is a remarkable weight loss (*ca.* 75%). The amount of residue is 16.5%. Assuming that the residual material of {Cr₁₀} is Cr₂O₃, the expected amount of Cr₂O₃ would be 35% of the starting weight. This loss of material and the straight jump at 450 °C suggest the possibility of – albeit non-quantitative – sublimation.

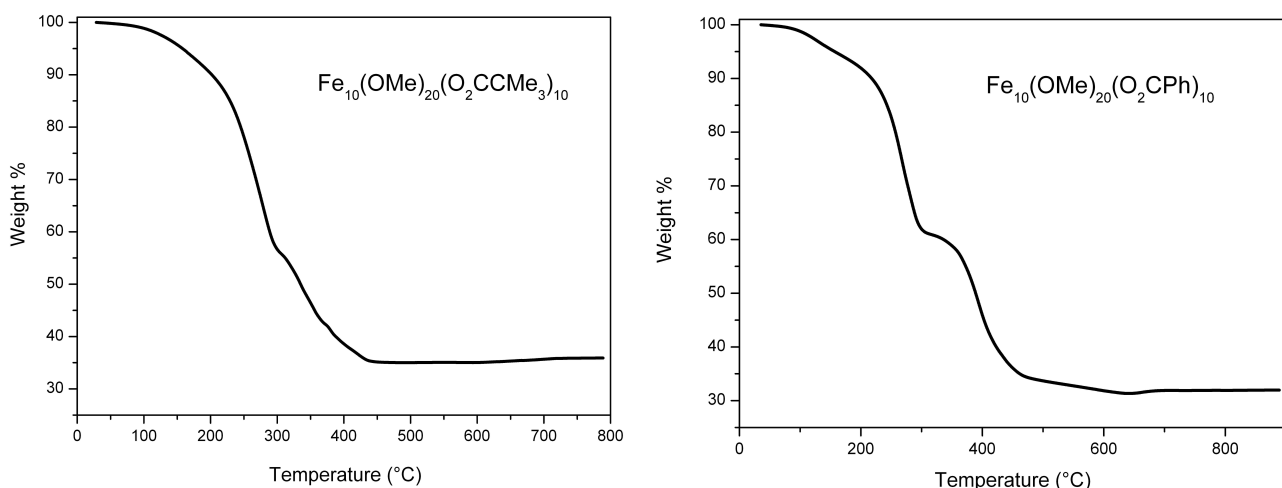


Fig. S5. TGA data for $\{\text{Fe}_{10}(\text{OMe})_{20}(\text{O}_2\text{CCMe}_3)_{10}\}$ and $\{\text{Fe}_{10}(\text{OMe})_{20}(\text{O}_2\text{CPh})_{10}\}$.

4. $\{\text{Cr}_{10}\}$ sub-monolayer deposition and characterization

The UHV system consists in an preparation chamber with a base pressure of 2×10^{-10} mbar containing equipment for sample sputtering, thermal annealing, molecular beam epitaxy, XPS and LEED analysis and connected to a second UHV chamber equipped with the STM stage.

4.1 Substrate preparation and $\{\text{Cr}_{10}\}$ deposition experimental details

An Ag (110) single crystal (MaTeck GmbH, Germany) was used as the substrate. It was cleaned by repeated cycles of 1 keV Ar^+ sputtering and annealing at 820 K until a clean surface with sufficiently large terraces was obtained, as confirmed by STM imaging.

Before the sublimation experiments, $\{\text{Cr}_{10}\}$ has been crystallized twice from toluene, than dissolved in hexane and vacuum-dried for 24 h in order to ensure high purity. $\{\text{Cr}_{10}\}$ molecules were deposited in UHV from an effusion cell (NTEZ-40, MBE Komponent). Few mg of $\{\text{Cr}_{10}\}$ were loaded into a Pyrolytic Boron Nitride crucible, whose temperature was raised to 510 K in approximately 4 hours and held at 525 K for 30 minutes in order to degas molecules. During the deposition the crucible was held at 510 K, the Ag substrate was kept at room temperature and the base pressure in the chamber was 5×10^{-10} mbar.

4.2 X-Ray Photoelectron Spectroscopy of $\{\text{Cr}_{10}\}$ sub-monolayer on the Ag(110) surface

XPS spectra in UHV were recorded on a monochromatized Gammascan Scienta spectrometer

(energy resolution 0.28 eV, measured at the Ag Fermi level) using a SES-100 electron analyzer, a MX650 Al K_α monochromatized X-ray source (1486.6 eV, 12KV, 270W). The sample analysis area was 0.5 mm in diameter and the working pressure was 3×10^{-10} mbar. The spectrometer was calibrated assuming the BE of the Ag3d_{5/2} line at 368.2 eV. A survey scan (Fig. S6) has been run in the 0-650 eV range to identify the chemical species present on the surface. Detailed scans were recorded for the C1s, O1s, Ag3p, Ag5d and Cr2p photo-peaks (Fig. S6, S7). Unfortunately, the Cr2p_{3/2} signal, centred at 577.4 eV, is partially overlapped with the very intense Ag3p peak of the silver substrate. This prevents us to perform chromium quantification, however it confirms the presence of Cr species on the surface. To prove the chemical integrity of the wheel we checked the atomic ratio of the ligands elements (C and O). The analysis involved Shirley-type background subtraction and, whenever necessary, spectral deconvolution, which was carried with the XPSPEAK 4.1 program. The atomic composition of the sample was calculated by peak integration. Integral peak areas were corrected for the atomic sensitivity factors.¹⁰ The experimental uncertainty on the reported atomic composition values does not exceed $\pm 5\%$. The results of the analysis are shown in Tables S5-S7: they are in very good agreement with the nominal values for {Cr₁₀}. Moreover, BEs for C1s, O1s, Cr2p_{3/2} are in agreement with the the results for the bulk wheel.

Table S5

{Cr ₁₀ } on Ag(110)	BE (eV)	FWHM (eV)
C1s (C _I + C _{II})	285.3	1.8
C1s (C _{III})	288.6	1.2
O1s	532.0	1.3
Ag3d _{5/2}	368.2	1.2
Ag3p _{3/2}	573.1	2.6
Cr2p _{3/2}	577.4	2.0

Table S5. XPS data recorded on a sub-monolayer of {Cr₁₀} on Ag(110).

Table S6

{Cr ₁₀ } on Ag(110)	BE (eV)	FWHM (eV)	% at.
C _I	285.0	1.2	59
C _{II}	286.1	1.2	27
C _{III}	298.6	1.1	14

Table S6. Deconvolution of C1s XPS peak recorded on a sub-monolayer of {Cr₁₀} on Ag(110).

Table S7

Atomic ratio	Nominal [§]	{Cr ₁₀ } on Ag(110)
C _{TOT} /O	1.75	1.73
C _I /C _{II}	2	2.1
C _{II} /C _{III}	2	1.9
C _I /C _{III}	4	3.9

[§]{Cr₁₀[OC_{II}H₃]₂₀[O₂C_{III}C_I(C_IH₃)₃]₁₀}

Table S7. Atomic ratio from XPS on a sub-monolayer of {Cr₁₀} on Ag(110).

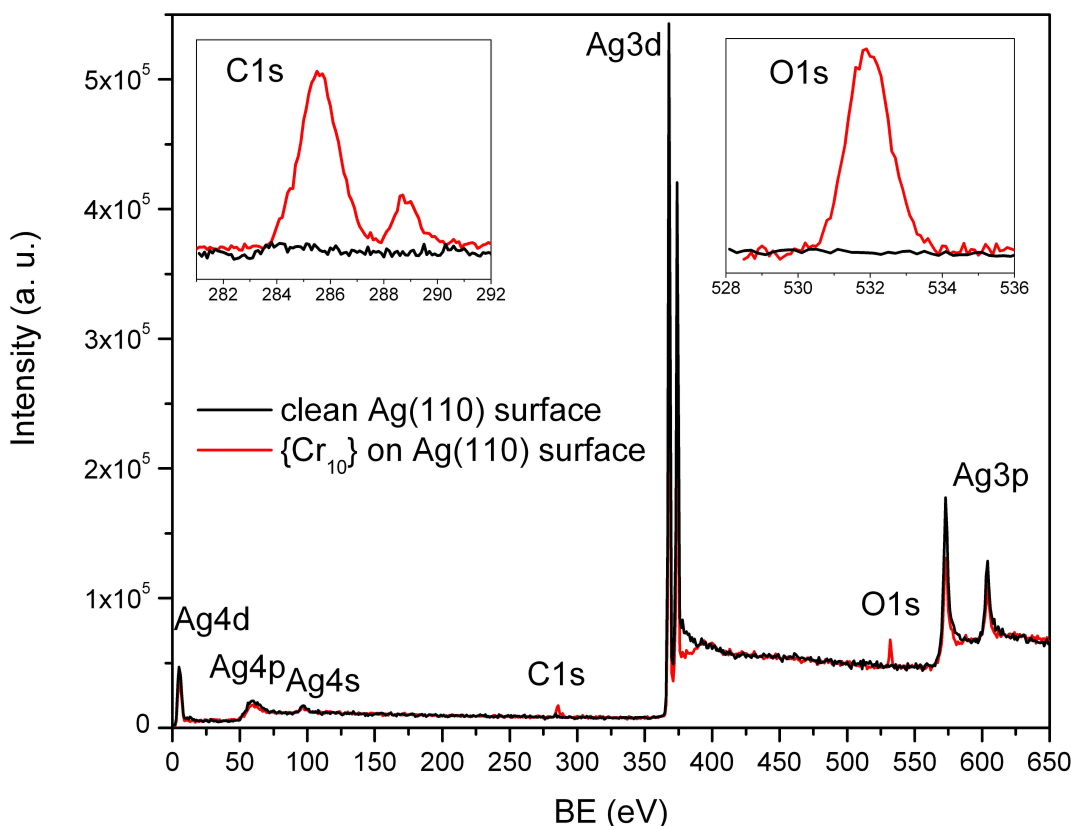


Fig. S6. XPS survey of the clean Ag (110) surface (black) and of the $\{Cr_{10}\}$ sub-monolayer on the Ag (110) surface (red); inset: O1s and C1s regions.

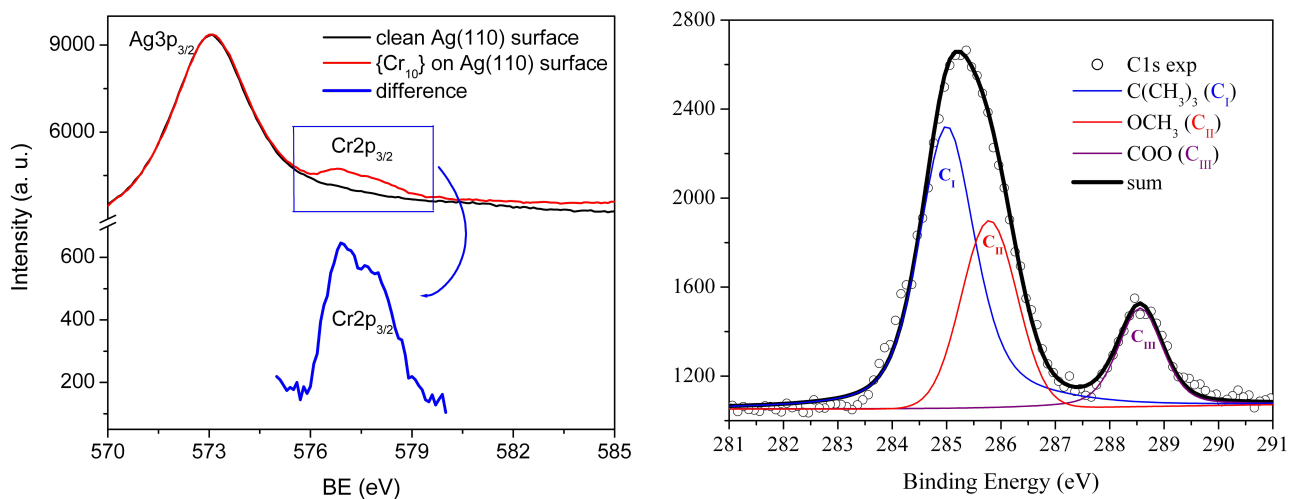


Fig. S7. On the left, $Ag3p_{3/2}$ and $Cr2p_{3/2}$ region of the clean Ag (110) surface (black) and of the $\{Cr_{10}\}$ sub-monolayer on the Ag (110) surface (red): the blue line is the difference spectrum in the 575-580 eV region. On the right, best fit profiles for C1s signal of the $\{Cr_{10}\}$ sub-monolayer on the Ag (110) surface.

4.3 Scanning Tunneling Microscopy experimental details

The STM measurements were carried out on an Omicron variable temperature (VT) STM stage: the sample was maintained at room temperature and the images were recorded in constant current mode, using a Pt-Ir tip obtained by electrochemical etching in aqueous solution. STM images were analyzed with the WSxM software.⁷ Sample bias and tunneling current values are reported throughout the paper. The scanner was calibrated in the z-direction with respect to the step edge of the clean Ag(110) surface. For the lateral calibration, Ag(110) rows along the [110] directions have been used.

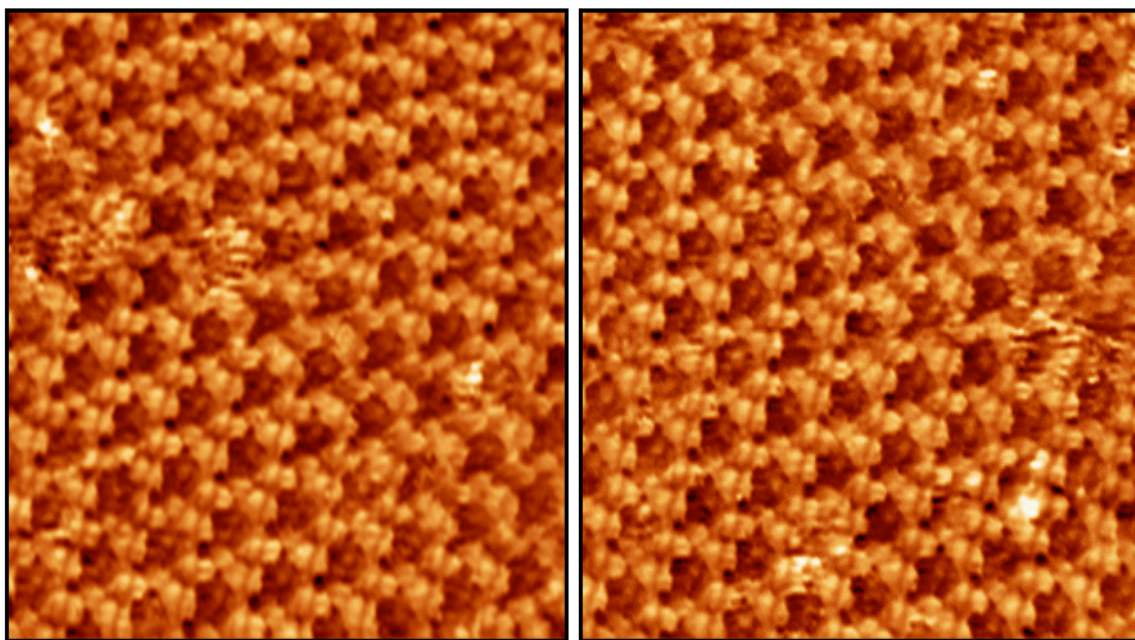


Fig. S8. High resolution STM images at opposite bias. On the left $20 \times 20 \text{ nm}^2$; -0.16 V; 0.15 nA; on the right $20 \times 20 \text{ nm}^2$; 0.16 V; 0.15 nA. The largely bias-independent nature of images features confirms their topographic rather than electronic origin.

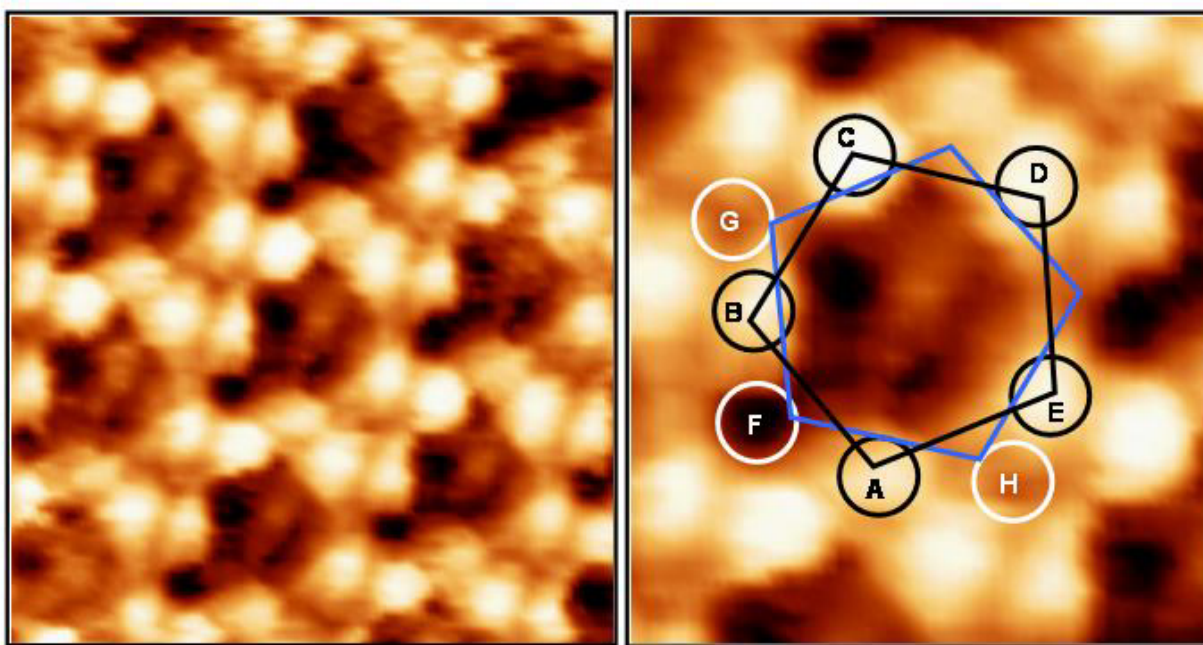


Fig. S9. On the left, high resolution STM image of Fig. 2b (article text). On the right, enlargement centred on the central molecule of the same image with sites labelling (see Table S8). Colour code: black labels refer to bright features corresponding to upward-pointing tert-butyl groups (black pentagon vertices) within a $\{\text{Cr}_{10}\}$ wheel, white labels refer to darker features close to the downward-pointing tert-butyl groups (blue pentagon vertices).

Table S8

Sites	Δz ($\pm 0.05 \text{ \AA}$)
B-A	0.20
C-A	0.36
D-A	0.38
E-A	0.28
G-F	0.32
H-F	0.27

Table S8. Height difference (Δz) between the labelled features suggesting a tilt of the molecular plane with respect to the surface.

5. References

1. M. Rancan, G. N. Newton, C. A. Muryn, R. G. Pritchard, G. A. Timco, L. Cronin and R. E. P. Winpenny, *Chem. Commun.*, 2008, 1560.
2. T. C. Stamatatos, A. G. Christou, S. Mukherjee, K. M. Poole, C. Lampropoulos, K. A. Abboud, T. A. O'Brien and G. Christou, *Inorg. Chem.*, 2008, **47**, 9021.
3. D. Low, G. Rajaraman, M. Helliwell, G. Timco, J. van Slageren, R. Sessoli, S. T. Ochsenbein, R. Bircher, C. Dobe, O. Waldmann, H. U. Güdel, M. A. Adams, E. Ruiz, S. Alvarez and E. J. L. McInnes, *Chem. Eur. J.*, 2006, **12**, 1385.
4. CrysAlisPro, *Oxford Diffraction Ltd.*, Version 1.171.34.36 (release 02-08-2010 CrysAlis171 .NET).
5. G. M. Sheldrick, *Acta Cryst.*, 2008, **A64**, 112.
6. O. V. Dolomanov, L. J. Bourhis, R. J. Gildea, J. A. K. Howard and H. Puschmann, *J. Appl. Cryst.*, 2009, **42**, 339.
7. I. Horcas, R. Fernandez, J. M. Gomez-Rodriguez, J. Colchero, J. Gomez-Herrero and A. M. Baro, *Rev. Sci. Instrum.*, 2007, **78**, 013705.
8. D. Briggs and M. Seah, Practical Surface Analysis 2nd Edn., Vol. 1, Auger and X-Ray Photoelectron Spectroscopy, Wiley, Chichester, 1990.
9. J. F. Moulder, W. F. Stickle, P. W. Sobol and K. D. Bomben, Handbook of X-ray Photoelectron Spectroscopy, Perkin-Elmer, Eden Prairie, MN, 1992.
10. C. D. Wagner, L. E. Davis, M. V. Zeller, J. A. Taylor, R. H. Raymond and L. H. Gale, *Surf. Interface Anal.*, 1981, **3**, 211.